DISTRIBUTION OF ORGANELLES AND MEMBRANES BETWEEN HEPATOCYTES AND NONHEPATOCYTES IN THE RAT LIVER PARENCHYMA

A Stereological Study

ANDRE BLOUIN, ROBERT P. BOLENDER, and EWALD R. WEIBEL

From the Department of Anatomy, University of Berne, Switzerland. Dr. Blouin's present address is the Faculty of Veterinary Medicine, University of Montreal, Saint-Hyacinthe, Quebec, Canada. Dr. Bolender's present address is the Department of Biological Structure, School of Medicine, University of Washington, Seattle, Washington 98195.

ABSTRACT

When biochemical studies on the liver are interpreted, the cells of the sinusoidal area frequently receive little attention because, compared to hepatocytes, their contribution to subcellular fractions is assumed insignificant. A systematic stereological analysis of liver parenchyma was therefore performed in order to determine the distribution of organelles and membranes between hepatocytic and nonhepatocytic cells, namely endothelial, Kupffer, and fat-storing cells. The livers were fixed by vascular perfusion and the data were corrected for systematic errors due to section thickness and compression. The extracellular space compartment includes the lumina of sinusoids (10.6%), the space of Disse (4.9%), and the bile canaliculi (0.4%). Hepatocytes constitute 78% of parenchymal volume; the nonhepatocytes account for 6.3% and consist of 2.8% endothelial cells, 2.1% Kupffer cells, and 1.4% fat-storing cells. The nonhepatocytes contribute 55% of the volume of lipid droplets in the liver, 43% of the lysosomes, and 1.2% of the mitochondria. Although the nonhepatocytes account for only 8% of the total surface area of parenchymal membranes, they contain 26.5% of all the plasma membranes, 32.4% of the lysosomal membranes, 15.1% of the Golgi apparatus, 6.4% of the endoplasmic reticulum, and 2.4% of the mitochondrial membranes.

The data demonstrate the extent to which nonhepatocytic organelles can potentially contaminate subcellular fractions used for biochemical studies. Particularly important for the interpretation of studies on lysosomes, plasma membrane, and Golgi apparatus is the finding that an appreciable part of these organelles may be derived from cell types other than hepatocytes.

When the results of biochemical studies on the liver are related to liver structure, it is often tacitly assumed that the role of cells other than hepatocytes can be ignored; accordingly, morphometric studies on liver cells have hitherto concentrated exclusively on hepatocytes (4, 17, 25, 34, 35). Hepatocytes are by far the most prominent component of liver parenchyma, in terms of both vol-

ume and membrane surface area; it is, however, not known what fraction of the various organelles or membranes of the liver is located in nonhepatocytes and may therefore appear as "contaminants" in subcellular fractions derived from homogenates.

Three types of nonhepatocytes are found in the liver parenchyma. Endothelial and Kupffer cells lining the sinusoids can be identified and distinguished in electron micrographs according to the characteristics established by Wisse (36–39). The fat-storing or stellate cells first described by Ito and Nemoto (14) do not participate in the actual lining of the sinusoid, but are rather associated with the space of Disse; they may be considered to represent a class of interstitial cells (5, 15, 20).

The objective of the present study was to assess the surface area of all membranes and the volume of all organelles present in liver parenchyma, and to determine their distribution among the four constituent cell types: hepatocytes, endothelial cells, Kupffer cells, and fat-storing cells. To this end, a systematic stereological analysis of electron micrographs of intact tissue samples derived from perfusion-fixed rat livers was performed.

MATERIALS AND METHODS

Perfusion Fixation

Male Sprague-Dawley rats, weighing 214 ± 5.8 g (Table I), were fasted for 24 h before the experiment. Deep anesthesia was induced by intramuscular injection of Hypnorm (fluanisone/fentanyl; 2 mg/kg body weight), after a 30-min pretreatment with Valium (Hoffman-LaRoche Inc., Nutley, N. J.) (7-chloro-1,3-dihydro-1-methyl-5-phenyl-2H-1,4-benzodiazepin-2-one) and Pethidin (pethidine hydrochloride).

A laparotomy was performed to expose the portal vein to which two loose ligatures were applied, one close to the liver, just before the vein bifurcates to form the left and right branches, and the other 1.5 cm distal to the first. The small afferent veins entering the portal vein within this 1.5 cm space were ligated, and the distal ligature was tightened. A polyethylene cannula (PE 90) was then introduced into the portal vein through a small incision and secured in place by tightening the proximal ligature. Perfusion was performed according to the method of Wisse (36), with the apparatus described by Gil and Weibel (11). Before the cannula was introduced, the perfusion pressure was adjusted to 20 mm Hg which subsequently fell to about 10 mm Hg during the perfusion, delivering 3–4 ml of fluid/min/100 g body weight. As soon as perfusion was established, the inferior vena cava was cut to allow for free drainage of the perfusate. To remove the blood, the liver was perfused at room temperature for 30 s with heparinized Ringer solution and for 5 min with 1.5% glutaraldehyde (Taab Laboratories, Reading, England), in a 0.05 M K-phosphate buffer, pH 7.4, 340 mosmol (adjusted with sucrose). When perfusion was completed, the liver was removed and weighed; the mean weight was 5.99 g (±0.15 SE), and liver volume as estimated by water displacement (23) was found to be 5.6 ml (±0.14).

Electron Microscopy

Thin slices of the left and medial lobes of the liver were cut into 0.5-mm cubes and postfixed for 2 h at 0–4°C with 1% osmium tetroxide buffered with 0.05 M cacodylate (pH 7.4, 340 mosmol [adjusted with sucrose]) and stained *en bloc* with uranyl acetate (4, 9). The tissue blocks were dehydrated in cold graded ethanols, carried through propylene oxide, and finally embedded in Epon (4, 18).

Silver-gray sections (~40 nm) were cut with a diamond knife on a Reichert ultramicrotome (American Optical Corp., Buffalo, N. Y.), mounted on 200-mesh grids covered with a carbon-coated parlodion film, and stained with lead citrate (22) for 20 min. Micrographs were recorded on 35-mm film with a Philips 300 electron microscope, contact printed, and finally projected × 10 onto test systems which allowed stereologial data to be collected by point counting methods (31, 33). The magnification was determined by including a micrograph of a calibration grating (Ernest F. Fullam, Inc., Schenectady, N. Y.) on each film strip.

Sampling Procedures

The stereological analysis was performed on five successfully perfused animals. The sampling procedure began with a random selection of 12 tissue blocks from each animal. A single section from each block provided seven micrographs, which were selected systematically (31, 33). Depending on the sampling requirements for a given magnification, either 6 or 12 blocks were used for a single animal, providing 42 or 84 micrographs, respectively.

Since four different magnifications were required to sample the liver components, the total number of micrographs per animal was 504 (12 films) and per five animals, 2,520 (60 films). For each morphological component being considered, a cumulative mean and standard error were calculated for each stereological parameter. The pooled point count data derived from three micrographs were used as the representative unit sample.

The stereological analysis required several sampling stages. In the first stage the volume densities of the various cell types and spaces related to liver parenchyma[1] were determined. The internal composition of each cell

[1] The liver parenchyma amounts to 92.4% of the total liver volume (D. Paumgartner, personal communication).

type was then estimated at higher magnification, using the individual cell volume as the reference space. When the volume density of each cell type in the liver parenchyma was known, the relative contribution of their organelles to the total aggregate population of these organelles in the parenchyma could be calculated. The details of this sampling procedure are described below.

Sampling Stage I

REFERENCE VOLUME: LIVER PARENCHYMA; MAGNIFICATION (FINAL) 7,500: The volume densities of the nonhepatocytic and hepatocytic compartments were related to the liver parenchyma. The nonhepatocytic compartment was subdivided into cells (endothelial, Kupffer, and fat-storing) and spaces (sinusoidal, Disse, and bile canalicular). 84 micrographs were analyzed per animal.

Sampling Stage II

REFERENCE VOLUME: LIVER PARENCHYMA; MAGNIFICATION (FINAL) 14,500: The surface density of the plasma membranes of endothelial, Kupffer, fat-storing cells, and hepatocytes was determined and related to the parenchymal volume. The plasma membrane of hepatocytes was subdivided into sinusoidal, lateral, and bile canalicular surfaces. Again, 84 micrographs were used per animal.

Sampling Stage III

REFERENCE VOLUME: CELL VOLUME BY TYPES; MAGNIFICATION (FINAL) 45,000: Volume densities were estimated for organelles found within endothelial, Kupffer, fat-storing cells, and hepatocytes.

Sampling Stage IV

REFERENCE VOLUME: CYTOPLASM OF INDIVIDUAL CELL TYPES; MAGNIFICATION (FINAL) 115,000: The final sampling stage was used to estimate surface densities of organelle membranes located within the cells listed in Stage III.

Stereological Methods

In all four sampling stages, a square, double lattice test system (1:9/36:324/4.5:1.5)[2] (33) with an area equal to 729 cm^2 was used to estimate volume and surface densities. Volume densities were estimated by counting test points lying over components and surface densities by counting the number of intersections occurring between membrane traces and test lines; both lineal components of the lattice were used. Formulas for calculating stereological parameters, as well as methods for integrating the data collected at different sampling stages, have been discussed in previous work from this laboratory (31, 33, 34). The point and intersection counts were collected with an electronic data recorder (32) and calculations were performed with a Hewlett-Packard 9830 A calculator (Hewlett-Packard Co., Palo Alto, Calif.).

[2] 1:9 is the ratio of coarse to fine points; 36:324 the number of coarse to fine points; 4.5:1.5 the length in cm of one of the two linear probes associated with each of the coarse and fine points.

Correction for Systematic Errors

Stereological estimates obtained directly from point counts are affected by two systematic errors: section compression and section thickness. These errors have been corrected according to the methods outlined in detail elsewhere (footnote 3). It has been found that sections were compressed to about 83% of their original dimension; the resulting overestimate of surface densities was corrected by the correction factor $Kc = 0.83$; volume densities are not affected by compression. Section thickness was estimated, by the fold method (24), to be 40 nm on the average. Correction coefficients for the section thickness effect for volume and surface densities, as shown in Tables II and III, were derived by the formulas of Weibel and Miles (footnote 4) for spherical, disk-shaped, and tubular elements (footnotes 3 and 5). The following extensions were necessary: the surface density estimate of plasma membrane of nonhepatocytes required no correction because the membrane was essentially composed of smooth sheets; pinocytotic vesicles were taken to have a diameter of 50 nm, yielding correction factors of 0.456 for V_V and 0.501 for S_V; in correcting S_V for lysosomal membranes, it was found that overprojection and truncation of caps cancelled one another so that no correction was required.

[3] Bolender, R. P., D. Paumgartner, G. Losa, and E. R. Weibel. Manuscript in preparation.

[4] Weibel, E. R., and R. E. Miles. Manuscript in preparation.

[5] A detailed description of the calculation of these correction factors would exceed the scope of this paper; it is included in a paper on correlated stereological analysis of intact liver cells and subcellular fractions (footnote 3) of which it is an important part. The general principle is as follows: (*a*) A geometric model is sought which approximately describes a given organelle; RER is considered to be built of an aggregate of thin circular disks, SER as an aggregate of tubules, whereby the disks and tubules are allowed to "interpenetrate," thus allowing for greatest generality of the stochastic process required for the modelling. (*b*) The fundamental formulas of Miles (19) permit the calculation of true surface density (S_V) of this model structure, as well as the apparent surface density (S_V'), when measured on a section of thickness T. (*c*) The correction coefficient is obtained as the ratio S_V/S_V'. The same procedure holds for volume density. (*d*) Organelles simulated by spherical vesicles are considered as discrete elements (without interpenetration), but a correction for the effect of cap loss due to grazing sections is included in this case.

RESULTS

Structure of Parenchyma and Stereological Model

Perfusion fixation provided a preservation of liver fine structure consistent with the requirements of this study: Disse and sinusoidal spaces were clearly delineated by extensions of endothelial and Kupffer cells, and the sinusoids were patent and practically free of blood cells and floccular material (Fig. 1). Endothelial, Kupffer, and fat-storing cells were well preserved and easily identified. The hepatocytes (Figs. 1–3) were also well fixed, although the glutaraldehyde prefixation preserved more of the matrix protein, resulting in a denser cytoplasmic "background" than usually found after osmium fixation alone (25, 34). As a consequence, the membranes appeared somewhat less contrasted.

The characteristic features of nonhepatocytes are shown in Figs. 2 and 3. Endothelial cells are smoothly apposed to the sinusoidal wall (Fig. 2); their perinuclear cytoplasm is thin and contains mainly some endoplasmic reticulum (ER), Golgi apparatus, and pinocytotic vesicles (Fig. 2). The broad cytoplasmic extensions of endothelial cells are poorly provided with organelles, but are frequently perforated by transendothelial channels (36), as shown in Fig. 2. Kupffer cells are attached to broad gaps in the endothelial lining (Fig. 3); they have no or only very short cytoplasmic extensions along the sinusoidal wall, but occasionally cytoplasmic flaps are seen to enwrap small bundles of fibrils (Fig. 3), as is observed for reticuloendothelial cells (13). The perinuclear cytoplasm of Kupffer cells is extensive and rich in organelles, typically containing a variety of lysosome-like inclusions of polymorphic shape and content (Figs. 1 and 3). Fat-storing cells are intercalated between hepatocytes and cells lining the sinusoid (Figs. 1 and 3); their stellate shape results from thin cytoplasmic extensions emanating from their cell body and extending into the Disse space beneath endothelial cells. Their typical inclusions are lipid droplets of homogeneous content (Fig. 3) which are usually enwrapped by a membrane (27–30).

The morphometric model in Fig. 4 shows how the total parenchymal space was divided into a hierarchical sequence of subcompartments, beginning with cell types and ending with their organelles. A similar model can be constructed for the relationship between the various classes of membranes in the four cell types. We shall call "total parenchymal membrane pool" the sum of all membranes in parenchymal cells and use it as a basic reference parameter for the distribution of membranes to the various cell and organelle classes.

In the perspective of the present study, we shall also use the aggregate volume of all organelles of a certain kind, e.g. mitochondria, as reference parameters, when we estimate the distribution of this organelle to the four cell types. We proceed similarly for membranes where the aggregate surface of the membranes of a certain class serves as reference parameter.

Volumetric Composition of Parenchymal Tissue

In the perfusion-fixed rat liver, nearly 16% of the parenchymal volume represents extracellular spaces which include the Disse space (4.9%), sinusoidal lumina (10.6%), and bile canaliculi (0.43%) (Table I and Fig. 5). The hepatocytes occupied 78% of the parenchymal volume, the nonhepatocytes 6% and the extracellular spaces taken together, 16%. Of the volume of nonhepatocytes, 44% were endothelial, 34% Kupffer, and 23% fat-storing cells.

In Table II and Fig. 5 the various types of parenchymal cells are compared with respect to their volumetric composition. The nucleus occupies as much as 20% of the volume of nonhepatocytes, whereas in hepatocytes it accounts for less than 10% of the cell volume. Mitochondria amount to 28% of the cell volume in the hepatocytes, but only to 4% in the nonhepatocytes. On the other hand, lysosomal granules (dense bodies) were found to be particularly abundant in Kupffer (14%) and endothelial cells (7%), but contributed only 0.8% to the volume of hepatocytes. Autophagic vacuoles were present in measurable quantities only in hepatocytes (0.23%) and, when added to the dense bodies, gave a total lysosomal compartment of 1.1%. Multivesicular bodies were measured separately only in fat-storing cells (0.7%); the very few found in hepatocytes were counted as "lysosomes." Lipid droplets were particularly frequent in fat-storing cells (25%), whereas they occupied less than 0.4% of the hepatocytic volume. It should be noted, however, that the 24-h fast might have affected the lipid stores in the liver. Pinocytotic vesicles accounted for 5.5% of the endothelial cell volume. However, since these vesicles have diameters approaching the section thickness, they were considerably overesti-

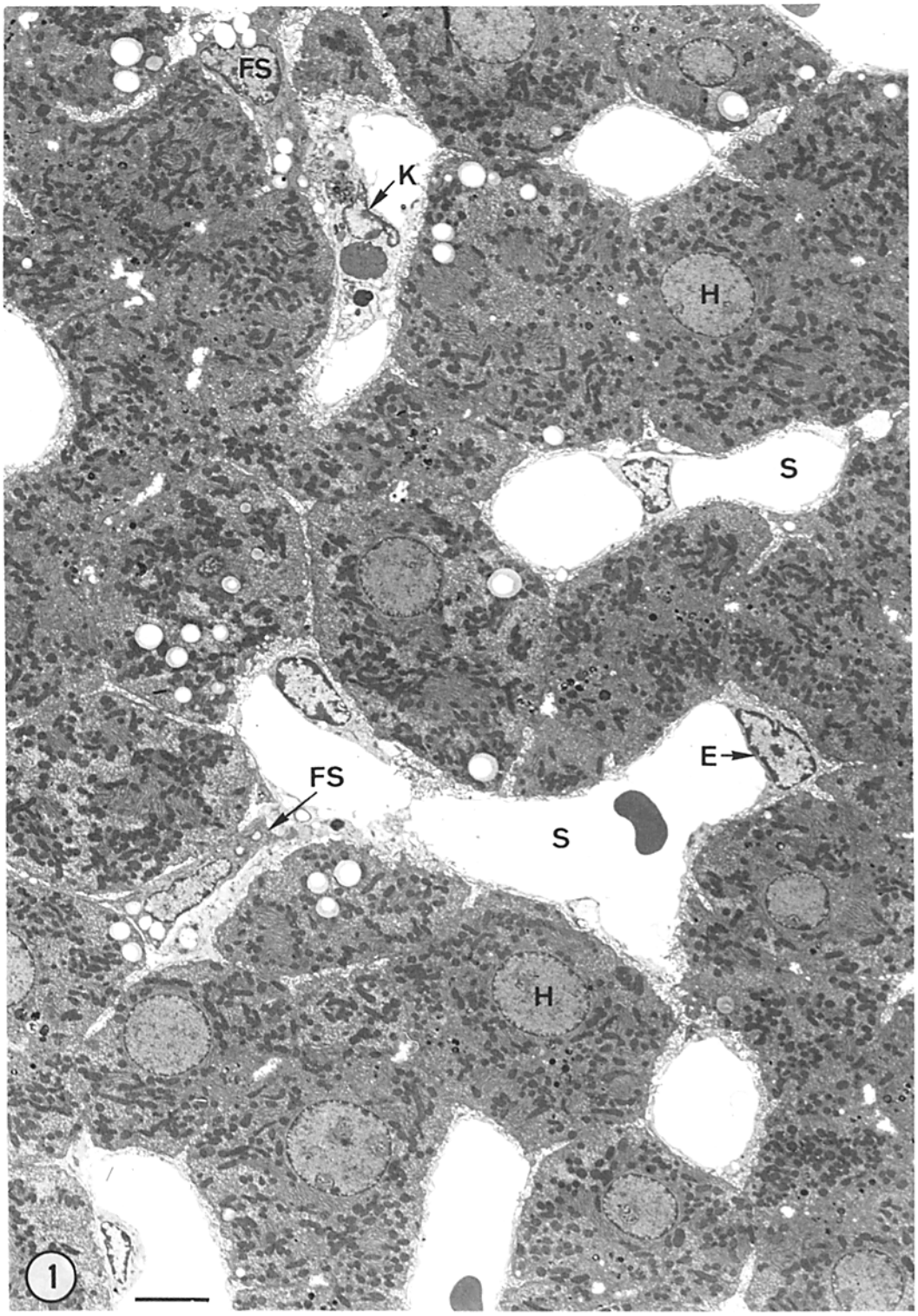

FIGURE 1 Low power electron micrograph of perfusion-fixed rat liver showing patent sinusoids (*S*), hepatocytes (*H*), endothelial cells (*E*), Kupffer cells (*K*), and fat-storing cells (*FS*). Magnification 2,100. Bar, 5 μm.

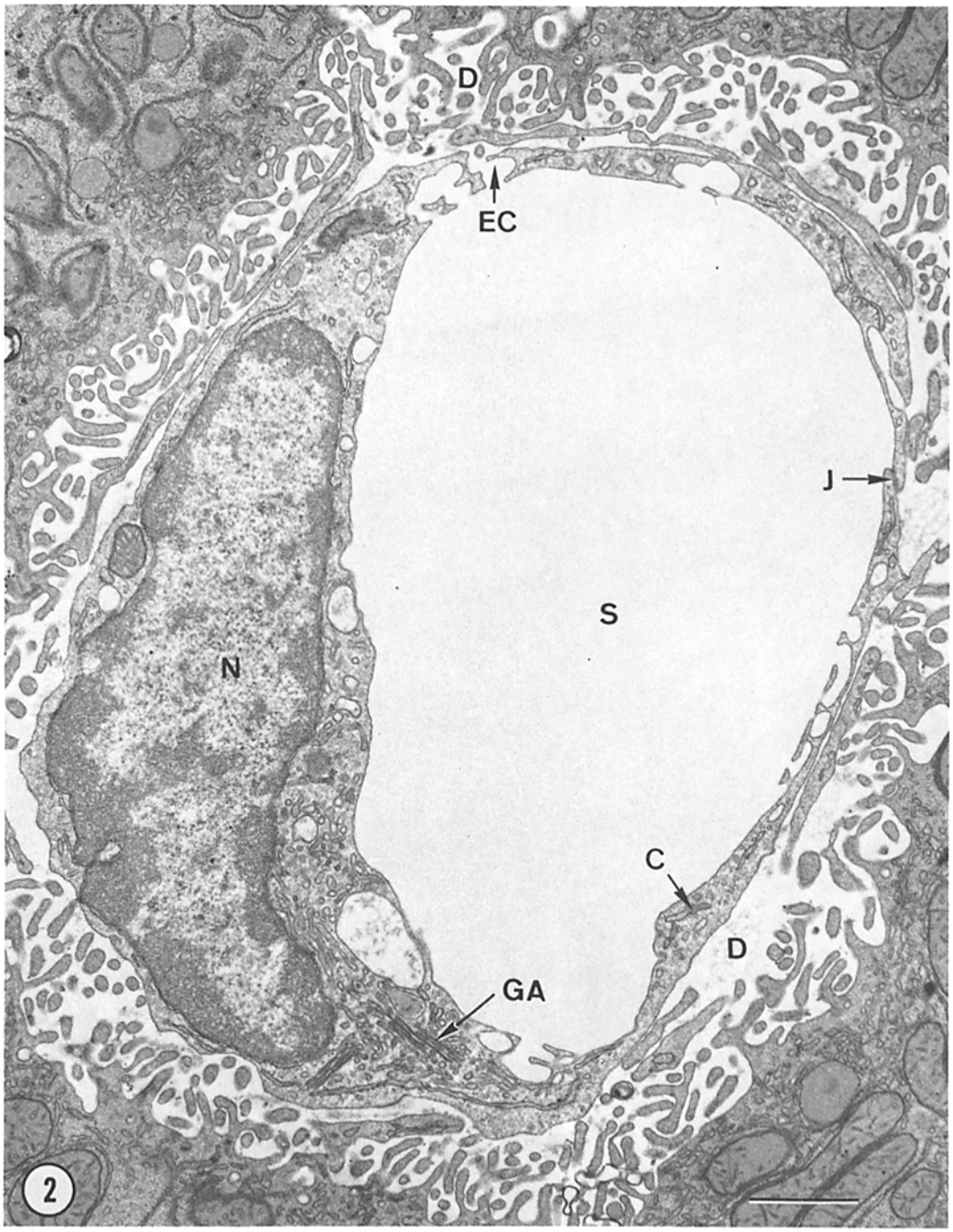

FIGURE 2 Endothelial cell from perfusion-fixed rat liver has flattened nucleus (*N*) and a well-developed Golgi apparatus (*GA*) in the perinuclear cytoplasm. Cytoplasmic extensions (*C*) line the sinusoidal space (*S*); they are joined by junctions (*J*) but are perforated by transendothelial channels (*EC*) that extend to the Disse space (*D*). Magnification 16,500. Bar, 1 μm.

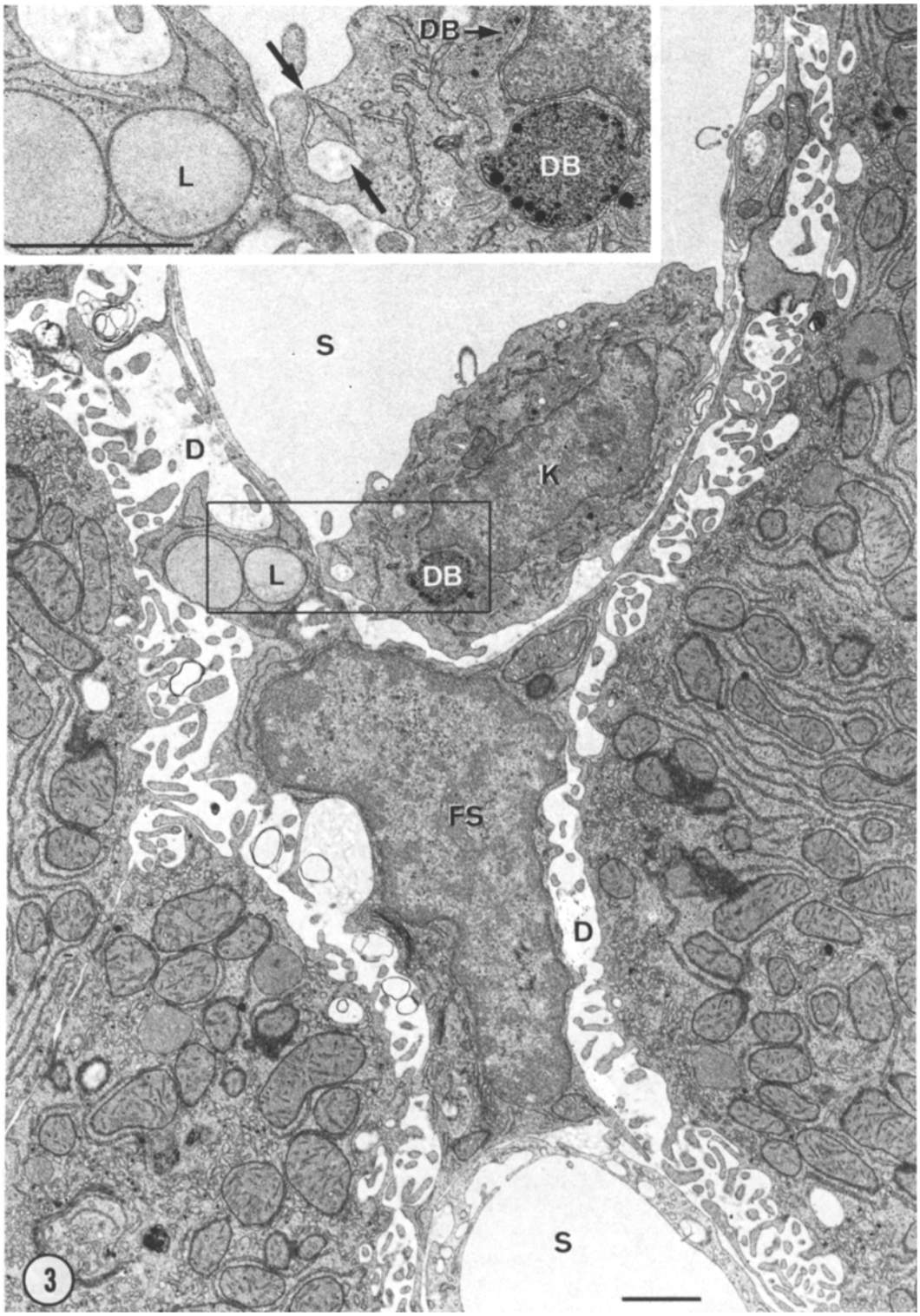

FIGURE 3 Kupffer cell (*K*) is devoid of lining cytoplasmic extensions; its abundant perinuclear cytoplasm contains dense bodies (*DB*). The fat-storing cell (*FS*) is associated with the Disse space (*D*) and contains spheroid lipid droplets enwrapped by a membrane. The inset shows Kupffer cell dense bodies (*DB*) and lipid droplets (*L*) of a fat-storing cell at higher power; it is also seen that Kupffer cells may envelop a fine connective tissue fiber with a cytoplasmic flap (arrows). Magnification 12,600; bar, 1 μm. Inset 28,000; bar, 1 μm.

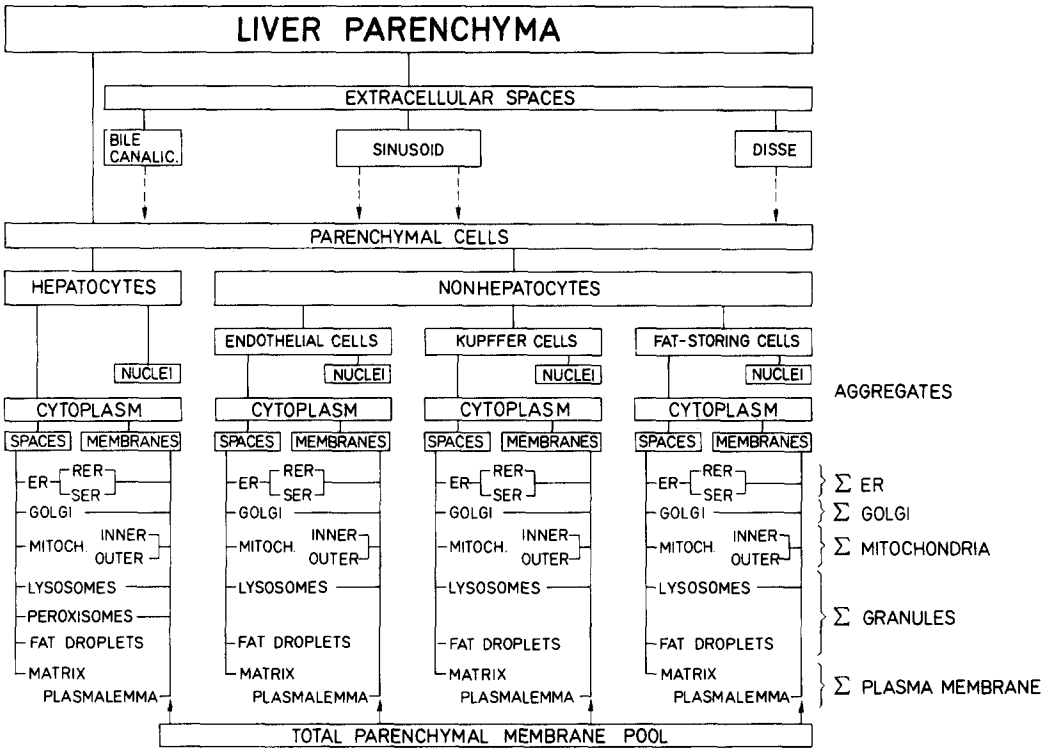

FIGURE 4 The morphometric model indicates how the total parenchymal volume (space) is divided into several compartments, including extracellular spaces, specific cell types, and organelles. Organelle volumes are expressed in terms of the total parenchymal volume as well as the volume of the different cell types. The "total parenchymal membrane pool" refers to the aggregate membrane surface area found in all parenchymal cells and is used as a reference for calculating the distribution of membranes among the various cells and organelles.

mated; when corrected for section thickness, their volume density falls to about 2.5%.

In Table IV and Fig. 7 the distribution of the organelles of a certain kind to hepatocytes and nonhepatocytes is given as percent of the aggregate organelle volume. Whereas nonhepatocytes contain only slightly more than 1% of the total mitochondrial population, their lysosomes and lipid droplets amount to as much as 38% and 55%, respectively.

Distribution of Organelle Membranes

Table III presents both the raw estimates for the membrane areas and those corrected for effects of section thickness and compression. The corrected data were used for calculating the percentage distributions, as presented in Table IV and in Fig. 6. Figures quoted in the text are corrected data.

The liver parenchyma contains a total membrane pool of 11.5 m^2/cm^3. Of this, over 92% is in hepatocytes; half of the nonhepatocyte membranes are in endothelial cells. The largest fractions of this membrane pool are the membranes of mitochondria (44%) and of ER (40%), of which 98% and 94%, respectively, are in hepatocytes.

It is evident from Fig. 6, however, that nonhepatocytes contain a comparatively large fraction of the plasma membranes (26.5%), more than half of this being associated with endothelial cells of the sinusoid. Of the hepatocyte plasma membranes, 72% are at the sinusoidal surface; this includes the membranes of the microvilli.

Section thickness has differently affected the estimates of the membrane area of the various classes of organelles (Table III); the error introduced depends on the shape and the relative dimensions of the components. Thus, in the raw estimate, smooth ER (SER) tubules appeared to make up 45% of the ER membranes; but, after section thickness correction, their part in the ER

TABLE I

Composition of Liver

	% of Parenchymal vol*
Nonhepatocytes	6.3 ± 0.49
Endothelial cells	2.8 ± 0.19
Nuclei	0.44 ± 0.08
Cytoplasm	2.36 ± 0.08
Kupffer cells	2.1 ± 0.31
Nuclei	0.39 ± 0.07
Cytoplasm	1.71 ± 0.07
Fat-storing cells	1.4 ± 0.19
Nuclei	0.28 ± 0.04
Cytoplasm	1.12 ± 0.04
Hepatocytes	77.8 ± 1.15
Nuclei	7.6 ± 0.50
Cytoplasm	70.2 ± 1.13
Intercellular spaces	15.9 ± 0.75
Disse space	4.9 ± 0.35
Sinusoidal lumen	10.6 ± 0.45
Biliary canaliculi	0.43 ± 0.05

* Mean ± 1 SE; N = 5.

membrane area fell to 37%. If Golgi membranes are considered part of the ER (6), they contribute 4% to ER membranes in the hepatocytes, but as much as 15% in endothelial cells.

Table IV and Fig. 7 show again how the aggregate membranes of a certain kind are distributed between hepatocytes and nonhepatocytes. Major nonhepatocyte parts are noticed for Golgi (15%) and lysosomal membranes (32%), as well as for plasma membrane. About 8% of the total membrane pool is in nonhepatocytes.

DISCUSSION

Previous morphometric studies on the liver have exclusively focussed on hepatocytes (4, 17, 34); it must, however, be expected that subcellular fractions derived from homogenized liver tissue will contain organelles and membranes derived from other cells as well, particularly from the nonhepatocytes of liver parenchyma. Such considerations were important in view of a parallel study in which we attempted to estimate, by means of stereological methods, how well organelles and membranes were recovered in subcellular fractions when compared to homogenate and to intact tissue (footnote 3). The present study was designed to provide information on the relative composition of hepatocytes and nonhepatocytes of rat liver parenchyma.

Methods

Nonhepatocyte of liver parenchyma are associated with the sinusoid and the Disse space. They are difficult to identify in exsanguinated tissue fixed by immersion, as it is available as tissue samples from livers used for homogenization (footnote 3). For the present study, therefore, we had to resort to fixation by vascular perfusion from the portal vein, since the patency of sinusoids permitted unambiguous differentiation of the

TABLE II

Volumetric Composition of the Different Cell Types

	Volume, %*			
	Per Cell		Per parenchyma	
Nuclei:				
Hepatocyte	9.8	± 0.64	7.6	± 0.5
Endothelial cell	16.4	± 2.65	0.46	± 0.074
Kupffer cell	19.2	± 2.07	0.40	± 0.043
Fat-storing cell	20.8	± 2.49	0.29	± 0.035
Cytoplasmic matrix:				
Hepatocyte	57.9	± 0.80	45.0	± 0.62
Endothelial cell	66.9	± 0.99	1.87	± 0.03
Kupffer cell	60.9	± 1.56	1.28	± 0.03
Fat-storing cell	48.4	± 3.1	0.68	± 0.04
Mitochondria:				
Hepatocyte	28.32	± 0.50	22.03	± 0.39
Endothelial cell	4.26	± 0.39	0.12	± 0.011
Kupffer cell	4.52	± 0.38	0.09	± 0.008
Fat-storing cell	4.36	± 0.50	0.06	± 0.007
Lysosomes:				
Hepatocyte	0.82	± 0.16	0.64	± 0.12
Endothelial cell	6.86	± 1.10	0.19	± 0.03
Kupffer cell	13.57	± 0.84	0.29	± 0.02
Fat-storing cell	0.23	± 0.04	0.003	± 0.0006
Multivesicular bodies:				
Fat-storing cell	0.73	± 0.076	0.01	± 0.001
Autophagic vacuoles:				
Hepatocyte	0.23	± 0.059	0.18	± 0.046
Peroxysomes:				
Hepatocyte	2.44	± 0.14	1.89	± 0.11
Lipid droplets:				
Hepatocyte	0.37	± 0.16	0.29	± 0.13
Fat-storing cell	25.34	± 2.85	0.35	± 0.04
Pinocytotic vesicles:‡				
Hepatocyte	0.18	± 0.021	0.140	± 0.016
	0.082		*0.071*	
Endothelial cell	5.50	± 0.78	0.150	± 0.02
	2.51		*0.077*	
Kupffer cell	1.80	± 0.26	0.040	± 0.006
	0.82		*0.020*	
Fat-storing cell	0.16	± 0.028	0.0022	± 0.0004
	0.073		*0.0011*	

* Mean ± SE; N = 5.

‡ Data corrected for section thickness effect indicated by italics.

TABLE III

*Membrane Surface Area in m^2/cm^3 of Liver Parenchyma**

	Hepatocyte	Endothelial cell	Kupffer cell	Fat-storing cell	Total membranes	Correction factors
Plasma membranes	0.825±0.02	0.140 ±0.003	0.0392±0.001	0.0652±0.003	1.070±0.02	0.822‡
	0.563	*0.116*	*0.0325*	*0.0541*	*0.765*	
Endoplasmic reticulum	5.507±0.16	0.197 ±0.015	0.110 ±0.015	0.0610±0.007	5.875±0.14	
	3.801	*0.134*	*0.0797*	*0.0448*	*4.060*	
Rough	3.021±0.15	0.102 ±0.012	0.076 ±0.012	0.0450±0.006	3.244±0.14	0.962
	2.412	*0.081*	*0.0606*	*0.0357*	*2.590*	
Smooth	2.486±0.16	0.095 ±0.008	0.034 ±0.004	0.0160±0.003	2.631±0.16	0.673
	1.389	*0.053*	*0.0191*	*0.0091*	*1.470*	
Mitochondria	5.930±0.38	0.074 ±0.008	0.0424±0.008	0.0310±0.006	6.077±0.04	
	3.825	*0.049*	*0.0271*	*0.0203*	*3.921*	
Outer membrane	1.630±0.11	0.025 ±0.003	0.0111±0.007	0.0095±0.007	1.676±0.11	
	1.300	*0.020*	*0.0088*	*0.0073*	*1.336*	0.961
Inner membrane	4.300±0.78	0.049 ±0.006	0.0313±0.006	0.0215±0.004	4.402±0.78	
	2.525	*0.029*	*0.0183*	*0.0126*	*2.585*	0.739
Golgi apparatus	0.260±0.07	0.036 ±0.005	0.0060±0.001	0.0040±0.0004	0.306±0.073	
	0.170	*0.024*	*0.0042*	*0.0025*	*0.201*	0.789
Lysosomes	0.084±0.019	0.015 ±0.001	0.0242±0.004	0.0011±0.0005	0.124±0.021	1.0
	0.070	*0.012*	*0.0201*	*0.0009*	*0.103*	
Pinocytotic vesicles	0.025±0.002	0.0194±0.002	0.0078±0.002	0.0003±0.00013	0.052±0.007	0.510
	0.011	*0.0083*	*0.0033*	*0.0001*	*0.022*	
Total membranes	2.631	0.482	0.230	0.163	13.504	
	8.440	*0.343*	*0.167*	*0.123*	*9.072*	

* Raw estimates are given as mean ± 1 SE. (n = 5); italic numbers are means corrected for section thickness and compression.
‡ Valid only for hepatocyte plasma membrane.

TABLE IV

Distribution of Organelles and Membranes between Cell Types of Liver Parenchyma

	Hepatocyte	Endothelial cell	Kupffer cell	Fat-storing cell	Total
% Aggregate organelle volume*					
Nuclei	86.8	5.3	4.6	3.3	100
Cytoplasm	93.2	3	2.3	1.5	100
Mitochondria	98.8	0.53	0.40	0.27	100
Lysosomes	57.0	16.9	25.8	0.27	100
Lysosomes‡	62.4	14.5	22.1	1.0	100
Peroxysomes	100	–	–	–	100
Lipid droplets	45.3	–	–	54.7	100
Pinocytotic vesicles	42.1	45.2	12.0	0.7	100
% Aggregate membrane surface area*					
Plasma membrane	73.5	15.2	4.3	7.1	100
Endoplasmic reticulum	93.6	3.3	2.0	1.1	100
RER	93.1	3.1	2.3	1.3	100
SER	94.5	3.6	1.3	0.6	100
Mitochondria	97.6	1.2	0.7	0.5	100
outer	97.3	1.5	0.7	0.5	100
inner	97.7	1.1	0.7	0.5	100
Golgi apparatus	84.9	11.9	2.0	1.2	100
Lysosomes	67.6	12.1	19.5	0.9	100
Pinocytotic vesicles	47.6	37.0	14.9	0.5	100

* Mean, N = 5.
‡ Including MVB and autophagic vacuoles.

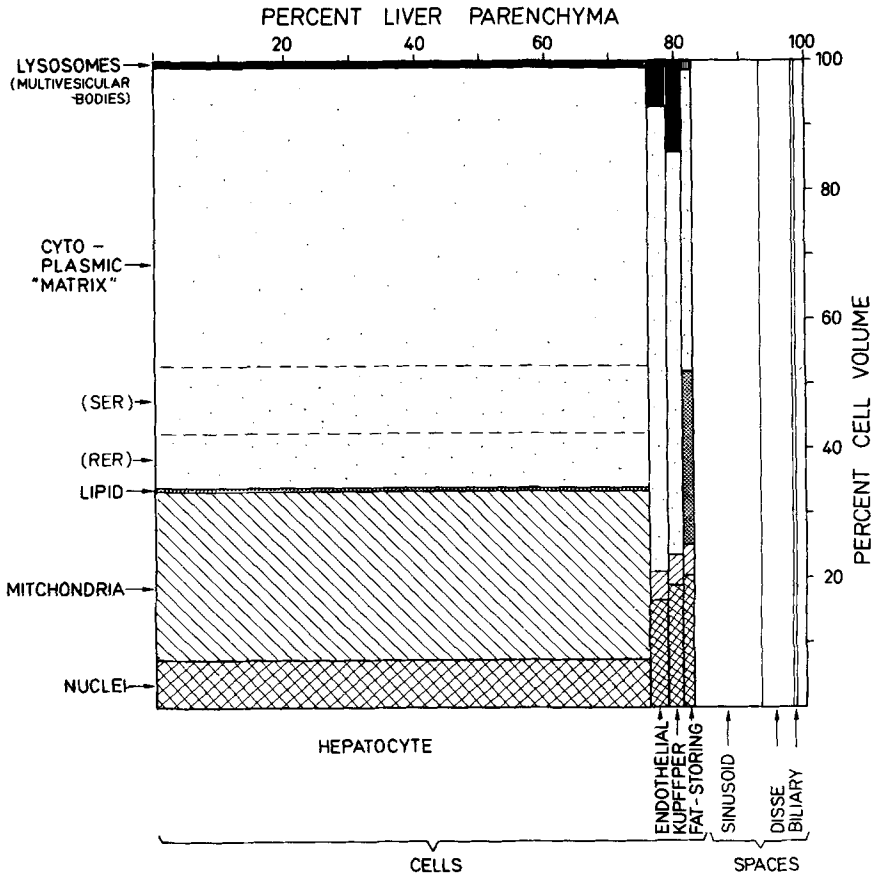

FIGURE 5 Volumetric composition of liver parenchyma.

three nonhepatocyte types. Because of this, the present data can only partly be compared to previous results, which were all obtained on immersion-fixed tissue. In particular, the extracellular spaces appear larger than after immersion fixation.

Perfusion pressure was rigorously controlled to approach that prevailing in the portal veins under physiological conditions. A comparison of our results on extracellular spaces with data obtained by physiological methods indicates that this was successfully achieved; thus, Reichen and Paumgartner (21) found, by a tracer dilution method, the space of Disse to be 5% of liver volume, which compares very well with our finding of 4.9%.

Stereological estimates on the membrane systems of cells have hitherto been affected by serious systematic errors due to section thickness and compression. Though recognized, these errors had to remain uncorrected because of a lack of reliable methods. Such a correction has now become possible; based on the integral geometric formulas of Miles (19), Weibel and Miles (footnote 4) have derived correction factors applicable to organelles whose shape can be described by spheres, thin disks, or tubules. The application of these formulas to the various classes of organelles and membranes of liver cells as well as the procedure for correcting section compression effects will be presented and discussed in detail elsewhere (footnote 3).

The effect of these corrections for section thickness and compression is revealed if the raw estimates presented in Table III are compared with the corrected data: the surface area of the total membrane pool in 1 cm^3 of liver parenchyma falls from 13.5 m^2/cm^3 (uncorrected) to 9.1 m^2/cm^3, i.e. to 67% of the uncorrected data. It is evident that this correction has affected the different components to a varying degree, because the correction factors depend on their shape.

Comparison with Other Data

Using light microscopy and immersion fixation,

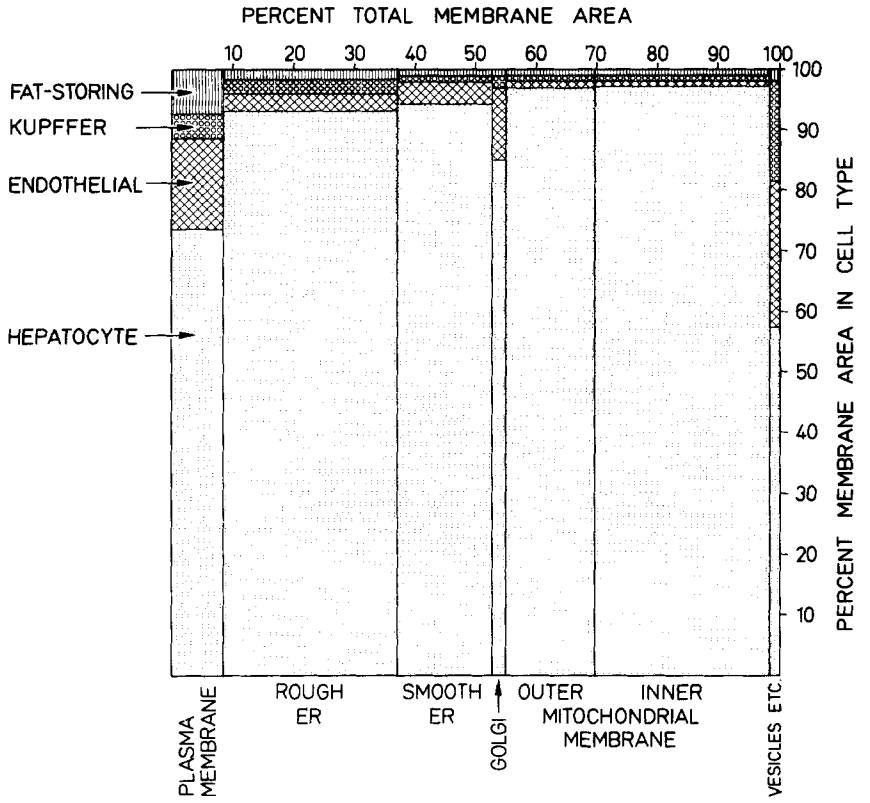

FIGURE 6 Distribution of the surface area of the various membrane classes to the four cell types (corrected data).

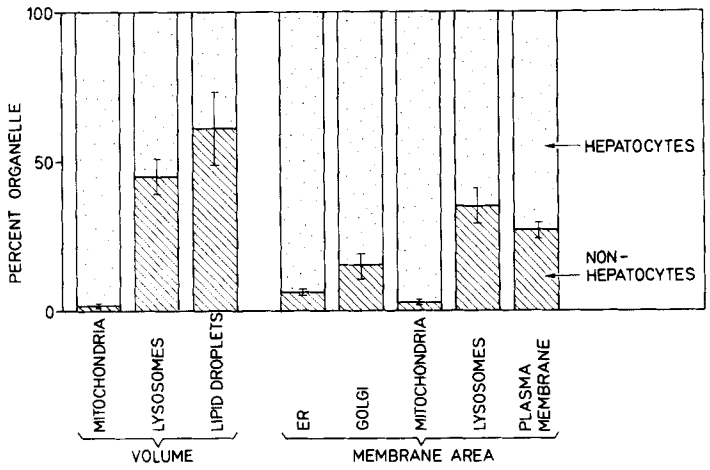

FIGURE 7 Distribution of aggregate of organelles and membranes to hepatocytes and nonhepatocytes.

Greengard et al. (12) estimated the volume densities of parenchymal cells in developing rat livers. Their values for adult animals (100 days postpartum) were 87% hepatocytes, 2% Kupffer cells, and 11% extracellular spaces. Similar estimates, found in Table I but derived from electron micrographs, were 78%, 2.1%, and 16%, respectively. Differences between the two studies probably re-

flect both the resolution of the microscopy and the different preparation methods.

The data on hepatocytes obtained in this study compare well with those found in the parallel study on rat livers fixed by immersion (footnote 3). After correction we found the surface density of ER to be 3.8 m^2/cm^3 parenchyma, as compared to 4.2 m^2/cm^3 in the other study. Considering that perfusion fixation resulted in a larger sinusoidal volume, the two estimates substantially agree. In both studies, rough ER (RER) amounted to 62% of the ER membrane surface. Excellent agreement was also found for mitochondrial membranes.

The reasons these estimates differ from those previously obtained in our laboratory (4, 25, 34) and by other investigators (17, 35) will be discussed in detail elsewhere (footnote 3). Reasons for the different estimates are mainly related to differences in the correction for section thickness and compression. The use of different magnifications ranging from 12,500 (17) to 60,000 (35) and 100,000 used in our laboratory may also have appreciably affected the estimates of membrane surface density, as was recently shown (16).

Potential Contribution of Nonhepatocytes to Organelle and Membrane Fractions

The main purpose of this study was to estimate to what degree nonhepatocytes could potentially contribute to the population of organelles that can be isolated by cell fractionation procedures. This estimation is based on the data presented in Table IV and on the assumption that both hepatocytes and nonhepatocytes are evenly disrupted during homogenization.

Slightly over 1% of the hepatic mitochondrial volume is in nonhepatocytes. Because the matrix is more abundant in most hepatocyte mitochondria than in those of other cells, and because nonhepatocyte mitochondria are considerably smaller, it is not surprising that as much as 2.5% of the mitochondrial membranes are in nonhepatocytes. In relative terms, the vast majority of liver mitochondria is derived from hepatocytes. In absolute terms, however, it must be noted that the total volume of nonhepatocytic mitochondria is as large as one quarter of the volume of all lysosomes in the liver, or is roughly of equal volume as hepatocytic lipid droplets. It is therefore not a negligible class of organelles.

Only 62% of the lysosomal granule volume is found in hepatocytes, 22% in Kupffer cells, and 14% in endothelial cells. Due to their different functional role (8, 26), lysosomes derived from these three cell types may well differ with respect to their composition; this may be one of the reasons for the heterogeneity of lysosomes observed in subcellular fractions by biochemical methods (1, 2, 14). The 1% "lysosomes" noted in fat-storing cells are mostly multivesicular bodies, a class of organelles that appears to be rare in other cell types in the liver. This is of particular interest because multivesicular bodies have been shown to play an important role in the synthesis of vitamin A in the fat-storing or stellate cells of the liver (27–30). Peroxisomes were observed exclusively in hepatocytes.

More than half of the hepatic lipid droplets are in "fat-storing" cells. It must be noted, however, that most of these droplets are clearly different from those found in hepatocytes: they are provided with a limiting membrane and their content appears of a homogeneous pale gray. Wake (30) has shown that these vesicles (type I lipid droplets) contain vitamin A rather than "fat" or triglycerides.

If we now turn to cytoplasmic membranes, we note that 94% of ER is in hepatocytes. However, ER membranes in nonhepatocytes amount to 0.26 m^2/cm^3 of liver parenchyma; this is one-third of the total surface of all plasma membranes, and 20% more than the total surface area of Golgi membranes. Of the latter, 15% are in nonhepatocytes, predominantly in endothelial cells. In view of the fact that recent methods for isolation and subfractionation of Golgi membranes (3, 7) exploit the presence of very low density lipoprotein particles (VLDL), it is noteworthy that nonhepatocyte Golgi cisternae are devoid of these particles; they would thus tend to go to the heavy subfraction GF3 (3, 7). In spite of their comparatively small relative volume, the nonhepatocytes contribute 26% of all the parenchymal plasma membrane. Finally, only about half of the membrane surface of small plasmalemmal vesicles (pinocytotic vesicles) is in hepatocytes, mostly beneath the sinusoidal and lateral plasma membrane; a large contribution of these vesicles derives from endothelial cells.

The present study has focussed on liver parenchyma and its cell population. One may evidently wonder whether the wall cells of larger blood vessels, the epithelium of bile ducts, etc. could be

further sources for contaminants. This cannot be excluded. However, of the 7% nonparenchymal volume, the major fraction is connective tissue and vessel lumina, so that less than 1% of the liver volume may represent nonparenchymatous cells.

The skillful assistance of Annette Larsen, Annemette Ohlsen, Gertrud Reber, and Karl Babl are gratefully acknowledged.

This study was supported by grants nos. 3.554.71 and 3.259.74 from the Swiss National Science Foundation. Dr. A. Blouin was recipient of a Postdoctoral Fellowship from the Canadian Medical Research Council.

Received for publication 24 May 1976, and in revised form 8 September 1976.

REFERENCES

1. BEAUFAY, H., D. S. BENDALL, P. BAUDHUIN, R. WATTIAUX, and C. DE DUVE. 1959. Tissue fractionation studies. 13. Analysis of mitochondrial fractions from rat liver by density-gradients centrifuging. *Biochem. J.* **73**:628–637.
2. BERG, T. and D. BOMAN. 1973. Distribution of lysosomal enzymes between parenchymal and Kupffer cells of rat liver. *Biochim. Biophys. Acta.* **321**:585–596.
3. BERGERON, J. J. M., J. H. EHRENREICH, P. SIEKEVITZ, and G. E. PALADE. 1973. Golgi fractions prepared from rat liver homogenates. II. Biochemical characterization. *J. Cell Biol.* **59**:73–88.
4. BOLENDER, R. P., and E. R. WEIBEL. 1973. A morphometric study of the removal of phenobarbital-induced membranes from hepatocytes after cessation of treatment. *J. Cell Biol.* **56**:746–761.
5. BRONFENMAJER, S., F. SCHAFFNER and H. POPPER. 1966. Fat-storing cells (lipocytes) in human liver. *Arch. Pathol.* **82**:447–453.
6. CLAUDE, A. 1970. Growth and differentiation of cytoplasmic membranes in the course of lipoprotein granule synthesis in the hepatic cell. I. Elaboration of the Golgi complex. *J. Cell Biol.* **47**:745–766.
7. EHRENREICH, J. H., J. M. BERGERON, P. SIEKEVITZ, and G. E. PALADE. 1973. Golgi fractions prepared from rat liver homogenates. I. Isolation procedure and morphological characterization. *J. Cell Biol.* **59**:45–72.
8. ESSNER, E., and A. B. NOVIKOFF. 1961. Localization of acid phosphatase activity in hepatic lysosomes by means of electron microscopy. *J. Biophys. Biochem. Cytol.* **9**:773–784.
9. FARQUHAR, M. G., and G. E. PALADE. 1965. Cell junctions in amphibian skin. *J. Cell Biol.* **26**:263–291.
10. FUTAI, M., P. K. TSUNG, and D. MIZUNO. 1972. Possible heterogeneity of the distribution of lysosomal marker enzymes among "lysosomal particles" of rat liver. *Biochim. Biophys. Acta.* **261**:508–516.
11. GIL, J., and E. R. WEIBEL. 1971. An improved apparatus for perfusion fixation with automatic pressure control. *J. Microsc. (Oxf.).* **94**:241–244.
12. GREENGARD, O., M. FEDERMAN, and W. E. KNOX. 1972. Cytomorphometry of developing rat liver and its application to enzymic differentiation. *J. Cell Biol.* **52**:261–272.
13. HUGHES, G. M., and E. R. WEIBEL. 1972. Similarity of supporting tissue in fish gills and the mammalian reticuloendothelium. *J. Ultrastruct. Res.* **39**:106–114.
14. ITO, T., and M. NEMOTO. 1952. Ueber die Kupfferschen Sternzellen und die "Fettspeicherungszellen" ("fat-storing cells") in der Blutkapillarenwand der menschlichen Leber. *Okajimas Folia Anat. Jpn.* **24**:243–258.
15. ITO, T., and S. SHIBASAKI. 1968. Electron microscopic study on the hepatic sinusoidal wall and the fat-storing cells in the normal human liver. *Arch. Histol. Jnp.* **29**:137–192.
16. KELLER, H. J., H. P. FRIEDLI, P. GEHR, M. BACHOFEN, and E. R. WEIBEL. 1975. The effects of optical resolution on the estimation of stereological parameters. Proceedings of the 4th International Congress for Stereology, Washington D.C. In press.
17. LOUD, A. V. 1968. A quantitative stereological description of the ultrastructure of normal rat liver parenchymal cells. *J. Cell Biol.* **37**:27–46.
18. LUFT, J. H. 1961. Improvements in epoxy resin embedding methods. *J. Biophys. Biochem. Cytol.* **9**:409–414.
19. MILES, R. E. 1975. On estimating aggregate and overall characteristic from thick sections by transmission microscopy. Proceedings of the 4th International Congress for Stereology, Washington D.C. In press.
20. NAKANE, P. K. 1963. Ito's fat-storing cell of the mouse liver. *Anat. Rec.* **145**:265–266.
21. REICHEN, J. and G. PAUMGARTNER. 1976. Uptake of bile acids by the perfused rat liver. *Amer. J. Physiol.* In press.
22. REYNOLDS, E. S. 1963. The use of lead citrate at high pH as an electron opaque stain in electron microscopy. *J. Cell Biol.* **17**:208–212.
23. SCHERLE, W. 1970. A simple method for volumetry of organs in quantitative sterology. *Mikroskopie.* **26**:57–60.
24. SMALL, J. V. 1968. Measurement of section thickness. Proceedings of the 4th European Conference for Electron Microscopy. 609–610.
25. STÄUBLI, W., R. S. HESS, and E. R. WEIBEL. 1969. Correlated morphometric and biochemical studies on the liver cell. II. Effect of phenobarbital on rat hepatocytes. *J. Cell Biol.* **42**:92–112.
26. THORBECKE, G. J., L. J. OLD, B. BENACERRAF, and D. A. CLARKE. 1961. A histochemical study of acid

and alkaline phosphatase in mouse livers during various conditions modifying activity of the reticuloendothelial system. *J. Histochem. Cytochem.* **9**:392–399.

27. WAKE, K. 1964. Distribution of vitamin A in the liver. Proceedings of the 5th Annual General Meeting of the Japanese Histochemical Association. 103.
28. WAKE, K. 1971. "Sternzellen" in the liver: perisinusoidal cells with special reference to storage of vitamin A. *Am. J. Anat.* **132**:429–462.
29. WAKE, K. 1973. Cytochemistry of the lipid droplets containing vitamin A in the liver. Proceedings of the 2nd International Symposium on Electron microscopy and cytochemistry. Drienerlo, The Netherlands. E. Wisse, W.Th. Daems, I. Molenaar, and P. van Duijn, editors. North-Holland Publishing Co., Amsterdam. 279.
30. WAKE, K. 1974. Development of vitamin A-rich lipid droplets in multivesicular bodies of rat liver stellate cells. *J. Cell Biol.* **63**:683–691.
31. WEIBEL, E. R. 1969. Stereological principles for morphometry in electron microscopic cytology. *Int. Rev. Cytol.* **26**:235–302.
32. WEIBEL, E. R. 1972. Current capabilities and limitations of available stereological techniques. II. Point counting methods. *In* Stereology 3. E. R. Weibel, G. Meek, B. Ralph, P. Echlin, and R. Ross, editors. Blackwell Scientific Publications, Oxford. 367–392.
33. WEIBEL, E. R., and R. P. BOLENDER. 1973. Stereological techniques for electron microscopic morphometry. *In:* Principles and techniques of electron microscopy. Vol. 3. M. A. Hayat, editor. Van Nostrand Reinhold Company, New York. 237–296.
34. WEIBEL, E. R., W. STÄUBLI, H. R. GNÄGI, and F. A. HESS. 1969. Correlated morphometric and biochemical studies on the liver cell. I. Morphometric model, stereologic methods, and normal morphometric data for rat liver. *J. Cell Biol.* **42**:69–91.
35. WIBO, M., A. AMAR-COSTESEC, J. BERTHET and H. BEAUFAY. 1971. Electron microscope examination of subcellular fractions. III. Quantitative analysis of the microsomal fraction isolated from rat liver. *J. Cell Biol.* **51**:52–71.
36. WISSE, E. 1969. An electron microscopic study of the fenestrated endothelial lining of rat liver sinusoids. *J. Ultrastruct. Res.* **31**:125–150.
37. WISSE, E. 1972. An ultrastructural characterization of the endothelial cell in the rat liver sinusoid under normal and various experimental conditions, as a contribution to the distinction between endothelial and Kupffer cells. *J. Ultrastruct. Res.* **38**:528–562.
38. WISSE, E. 1974. Kupffer cell reactions in rat liver under various conditions as observed in electron microscope. *J. Ultrastruct. Res.* **46**:499–520.
39. WISSE, E. 1974. Observations on the fine structure and peroxidase cytochemistry of normal rat liver Kupffer cells. *J. Ultrastruct. Res.* **46**: 393–426.